BIOLOGY OF REPRODUCTION (2014) **90**(3):52, 1–11
Published online before print 22 January 2014.
DOI 10.1095/biolreprod.113.115337

Integral Proteomic Analysis of Blastocysts Reveals Key Molecular Machinery Governing Embryonic Diapause and Reactivation for Implantation in Mice[1]

Zheng Fu,[5,6,7] Bingyan Wang,[5,6] Shumin Wang,[5,6] Weiwei Wu,[5,6,7] Qiang Wang,[6] Yongjie Chen,[6,7] Shuangbo Kong,[6,7] Jinhua Lu,[6,7] Zhenzhou Tang,[6] Hao Ran,[6] Zhaowei Tu,[6,7] Bo He,[6,7] Shuang Zhang,[6] Qi Chen,[6] Wanzhu Jin,[8] Enkui Duan,[6] Hongmei Wang,[6] Yan-ling Wang,[6] Lei Li,[6] Fengchao Wang,[4,9] Shaorong Gao,[3,9] and Haibin Wang[2,6]

[6]*State Key Laboratory of Reproductive Biology, Institute of Zoology, Chinese Academy of Sciences, Beijing, People's Republic of China*
[7]*Chinese Academy of Sciences, Beijing, People's Republic of China*
[8]*Key Laboratory of Animal Ecology and Conservation Biology, Institute of Zoology, Chinese Academy of Sciences, Beijing, People's Republic of China*
[9]*National Institute of Biological Sciences, Beijing, People's Republic of China*

ABSTRACT

Among nearly 100 mammalian species, implantation can be suspended at blastocyst stage for a certain time and reactivated under favorable conditions, a phenomenon known as embryonic diapause. Until now, the underlying molecular mechanism governing embryonic diapause and reactivation for implantation remained largely unknown. Here we conducted the first integral proteomic analysis of blastocysts from diapause to reactivation by using a physiologically relevant mouse delayed implantation model. More than 6000 dormant and reactivated blastocysts were used for the proteomic analysis. A total of 2255 proteins were detected. Various cellular and molecular processes, including protein translation, aerobic glycolysis, pentose phosphate pathway, purine nucleotide biosynthesis, glutathione metabolism, and chromatin organization were identified as differentially regulated. In particular, we demonstrated a remarkable activation of mitochondria in blastocysts upon reactivation from dormancy, highlighting their essential physiological significance. Moreover, the activities of the endosome–lysosome system were prominently enhanced in the mural trophectoderm of reactivated blastocysts, accompanied by active phagocytosis at the fetal-maternal interface, suggesting a critical role in promoting trophoblast invasion. Collectively, we provided an integral proteomic view upon the regulatory network of blastocyst reactivation from diapause, which will help to better interpret the nature of embryonic diapause and reactivation in wild animals and to identify molecular indicators for selecting blastocysts with high implantation competency.

blastocyst reactivation, embryonic diapause, implantation, proteome

INTRODUCTION

Successful implantation requires synchronization of the blastocyst to achieve implantation competency and the uterus to enter the receptive state. This embryo-uterine dialog during implantation is divided into three stages: apposition, attachment, and penetration. In mice, blastocyst becomes closely apposed to the uterine luminal epithelium at the antimesometrial pole during apposition. It is followed by trophectoderm cells physically and physiologically attaching to the uterine luminal epithelium. Subsequent penetration involves the invasion of blastocyst through the luminal epithelium and basal lamina into the stroma [1]. However, these sequential events in mice can be experimentally suspended by ovariectomy before the preimplantation ovarian estrogen secretion and maintained by injection of progesterone, a condition known as embryonic diapause or delayed implantation during which the blastocyst remains quiescent and the embryo-uterine attachment does not occur [2, 3]. In fact, this phenomenon has been observed in nearly 100 species of mammals as an evolutionary strategy to ensure successful reproduction [4–8]. The state of embryonic diapause in wild mammals can be terminated and then initiated so implantation occurs under favorable conditions such as appropriate temperature, length of daylight, and sufficient nutrients [6].

In regard to the molecular machinery governing timely blastocyst implantation, although uterine receptivity has been extensively explored, with identification of a wide range of regulatory molecules [9, 10], most previous studies have focused on revealing the cellular activities during blastocyst dormancy and termination of dormancy [11]. The molecular basis governing blastocyst reactivation from diapause for implantation remains largely unknown. In this respect, a global molecular view distinguishing dormant from reactivated blastocysts in mice was first achieved by a previous microarray analysis [12]. However, only approximately 229 differentially

[1]Supported in part by the National Basic Research Program of China (2011CB944400 to H.B.W.), the National Natural Science Foundation (81130009 and 81330017 to H.B.W.), and the Strategic Priority Research Program of the Chinese Academy of Sciences (XDA01010103 to L.L.).
[2]Correspondence: Haibin Wang, State Key Laboratory of Reproductive Biology, Institute of Zoology, Chinese Academy of Sciences, 1 Beichen West Road, Chaoyang District, Beijing 100101, PR China.
E-mail: hbwang@ioz.ac.cn
[3]Correspondence: Shaorong Gao, National Institute of Biological Sciences, 7 Science Park Rd., ZGC Life Science Park, Beijing 102206, PR China. E-mail: gaoshaorong@nibs.ac.cn
[4]Correspondence: Fengchao Wang, National Institute of Biological Sciences, 7 Science Park Rd., ZGC Life Science Park, Beijing 102206, PR China. E-mail: wangfengchao@nibs.ac.cn
[5]These authors contributed equally to this work.

Received: 29 October 2013.
First decision: 27 November 2013.
Accepted: 17 January 2014.

eISSN: 1529-7268 http://www.biolreprod.org
ISSN: 0006-3363

expressed genes were identified. A deeper insight into the molecular mechanism governing the achievement of blastocyst implantation competency warranted further investigation.

In the present study, we used the physiologically relevant mouse delayed implantation model combined with high-throughput liquid chromatography-tandem mass spectrometry (LC-MS/MS) approach to analyze the global protein profiles in blastocysts at dormancy versus at reactivation. Our proteomic analysis highlighted a dynamic activation of mitochondria-related energy metabolism and endosome–lysosome system function during blastocyst reactivation from dormancy.

MATERIALS AND METHODS

Animal Use and Embryo Collection

Adult CD-1 male and female mice were used in the present study. Mice were housed in the Institutional Animal Care Facility of the Institute of Zoology according to institutional guidelines for laboratory animals. The animal use protocol was approved by the institutional Animal Care Committee of the Institute of Zoology. The dormant and reactivated blastocysts were collected as previously described [2]. Female mice were ovariectomized on the morning of Day 4 (0800–1000 h) of pregnancy (Day 1 = vaginal plug) and injected daily with progesterone (2 mg per mouse) from Days 5–7. Dormant blastocysts were collected by flushing the uteri with Chatot-Ziomek-Bavister (CZB) medium on the morning of Day 8. For reactivated blastocysts, progesterone-primed implantation-delayed pregnant mice were killed 12–14 h after injection of estradiol-17β on Day 7. Blastocysts were rapidly frozen with liquid nitrogen and stored at −80°C until used for soluble protein extraction. More than 6000 blastocysts were collected for the LC-MS/MS analysis.

Proteome Analysis

Methods for protein extraction, digestion, and LC-MS/MS analysis were described previously [13]. In brief, tandem mass spectra were searched against European Bioinformatics Institute International Protein Index mouse protein database, using the ProLuCID protein database search algorithm. ProLuCID search results were then filtered with DTA Select version 2.0 using a cutoff of 1% for peptide false identification rate (−fp 0.01). Peptides with a Z score <4 (i.e., 4 standard deviations away from the average) or delta mass >7 ppm (−DM 7) were rejected. Furthermore, the minimum number of peptides needed to identify a protein was set to 1 (−p 1). Spectral counts for each protein were extracted from DTA Select files and downloaded into Excel (Microsoft) spread sheets and normalized to the total spectra counts of the sample from which a protein was identified. Functional classifications of the total and specific expressed proteins were done by the method called Argot2 (Annotation Retrieval of Gene Ontology Terms; http://www.medcomp.medicina.unipd.it/Argot2). Functional classification (Gene Ontology and KEGG pathways) of differentially expressed proteins (criteria were a fold change ≥1.5 and a spectrum count number ≥4) were done online using DAVID (DAVID Bioinformatics Resources 6.7; http://david.abcc.ncifcrf.gov/tools.jsp) and the KEGG pathway database (http://www.genome.jp/kegg/pathway.html). Cytoscape software was used to draw pictures. Protein identification using the ProLuCID program was conducted in the National Institute of Biological Sciences, Beijing.

Quantitative Real Time-PCR

Approximately 50–100 blastocysts for each group were used to extract RNA and obtain reverse transcription reactions. Expression levels of different genes were validated by quantitative real-time PCR analysis (ABI7500 sequence detector system; Applied Biosystems) according to the manufacturer's instructions. All primers for real-time PCR are listed in Supplemental Table S1 (all Supplemental Data are available online at www.biolreprod.org). All real-time PCR experiments were repeated at least 3 times.

Immunofluorescence Staining of Blastocysts

To localize ATP5B, CTSB, CTSD, H3K4me3, H3K9me3, H3K27me3, MCT4, CBX3, CBX5, and p-H2AFX, immunofluorescence staining of blastocysts was performed as previously described [14]. Immunofluorescence was captured by confocal scanning laser microscopy (LSM 710 model; Zeiss) as previously described. Antibodies specific to ATP5B (Santa Cruz), CTSB (Abcam), CTSD (Epitomics), H3K4me3 (Epitomics), H3K9me3 (Epitomics), H3K27me3 (Epitomics), MCT4 (Anbo), CBX3 (Anbo), CBX5 (Anbo), and p-H2AFX (Cell Signaling) were used.

Western Blotting for Blastocysts

Western blotting of candidate proteins was conducted as previously described [15]. Approximately 100 blastocysts for each group of samples were boiled in 5× loading buffer for 5 min. Then protein samples were electrophoresed using 10% SDS-polyacrylamide gels and transferred onto polyvinylidene difluoride membranes (Millipore). After the transfer, membranes were blocked with 5% skim milk in Tris buffered saline with 0.1% Tween-20 (TBST) for 2 h at room temperature and incubated overnight with primary antibodies in TBST. Antibodies to CTSB (Abcam), CTSD (Epitomics), and β-actin (Sigma) were used. After incubation with primary antibody, membranes were washed in TBST 3 times and then incubated with specific secondary antibodies (Zhongshan Golden Bridge Biotechnology Co., Ltd.) in 5% skim milk for 2 h at room temperature. Bands were visualized using chemiluminescent substrate (Supersignal West Pico; Thermo Scientific) according to the manufacturer's instructions.

TMRE Staining of Mitochondrial Membrane Potential

Dormant or reactivated blastocysts were washed with Whitten medium 3 times rapidly and then stained with tetramethylrhodamine ethyl ester (TMRE; Sigma) diluted 1:5000 within 30 min. Live imaging was accomplished by confocal microscopy (LSM710 model; Zeiss), by detecting fluorescence signals at 590 nm every 5 min. For live imaging, blastocysts were cultured in a 25-μl microdroplet and covered with mineral oil.

Detection of ATP Content

ATP contents of blastocysts were measured using a bioluminescence detection kit for ATP (Enliten ATP assay system; product FF2200; Promega). Approximately 10–20 blastocysts were used for detection in each batch. All detection experiments were repeated at least 3 times.

Detection of Glutathione Content

Glutathione (GSH) content of blastocysts was measured by using a GSH-Glo assay kit (product V6911; Promega). Approximately 20–50 blastocysts were used for each batch of detection. All detection experiments were repeated at least 3 times.

Transmission Electron Microscopy Scanning of Blastocysts or Implantation Sites

Transmission electron microscopy scans were carried out as previously described [16]. Blastocysts or implantation sites were rapidly fixed with 2% glutaraldehyde-PBS solution overnight (for blastocysts) or for 2 days (for implantation sites). Then they were washed with PBS several times and fixed with 1% osmic acid in PBS for 2 h. After dehydration and infiltration, blastocysts or implantation sites were embedded in JB-4 epoxy resin for semithin and ultrathin resin histology according to the manufacturer's instructions (Electron 25; Microscopy Sciences). Sections (semithin = 2 μm, ultrathin = 70–100 nm) were then cut using glass knives on a microtome (model RM2265; Leica). Semithin sections were stained with toluidine blue (Amresco), and ultrathin section contrast was developed with uranyl acetate and lead citrate staining.

RESULTS

Proteomic Analysis Reveals Dynamic Molecular Regulatory Network During Blastocyst Dormancy and Reactivation

To achieve high-resolution proteomic profiles of blastocysts, dormant and reactivated blastocysts were harvested by using the mouse delayed implantation model as previously described [2, 3]. The gross morphologies of dormant and reactivated blastocysts were distinguished as shown in Figure 1A. Mural trophectoderm cells of reactivated blastocysts showed signs of attachment to the uterine epithelium. Approximately 3000 dormant blastocysts and 3063 reactivated blastocysts were collected for mass spectrometry analysis (LTQ Orbitrap). As illustrated in Supplemental Tables S2 and

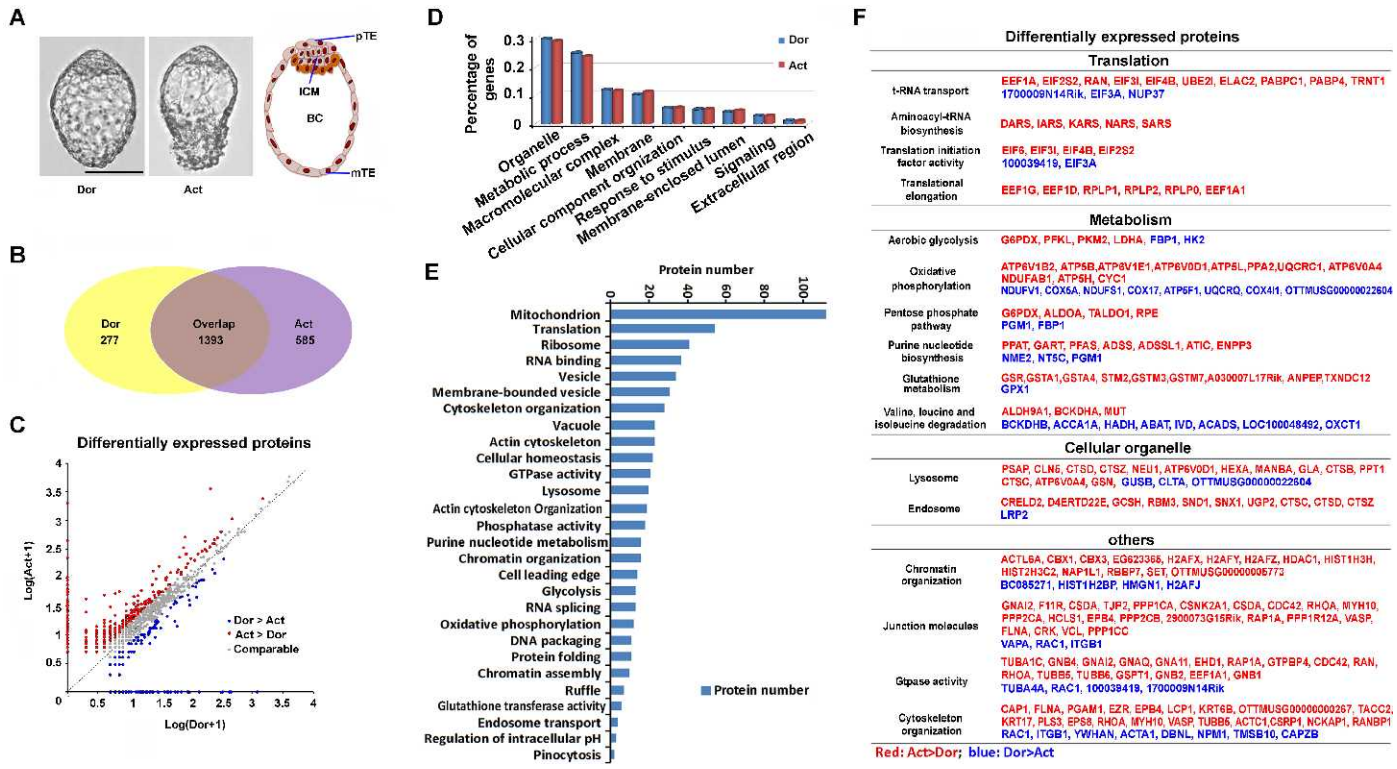

FIG. 1. Proteomic analysis of dormant and reactivated blastocysts is shown. **A**) Morphology of dormant (Dor) and activated (Act) blastocysts is shown. BC = blastocyst cavity; ICM = inner cell mass; mTE = mural trophectoderm; pTE = polar trophectoderm. Bar = 50 μm. **B**) Summary of total identified proteins is shown in the protein profiles, with 1978 in the activated blastocyst and 1670 in the dormant blastocyst. **C**) A scatter plot shows the total identified proteins according to their peptide spectrum counts, containing 419 proteins highly expressed in activated blastocysts (red) and 180 proteins highly expressed in dormant blastocysts (blue), and comparably expressed proteins (gray), respectively. Fold change ≥ 1.5; x- and y-axes indicate the value of $\log_2$ (spectrum count of specific protein + 1). **D**) Proportions of total detected proteins annotated to various cellular compartments and biological processes showed similar patterns between dormant and activated blastocysts. **E**) Gene Ontology analysis of the 599 differentially expressed proteins showed enrichment of proteins to mitochondria function, ribosome, chromatin organization, endosome, lysosome, and so on. **F**) Detail shows differentially expressed proteins in diverse categories according to gene ontology and KEGG pathway analyses.

S3, we successfully identified 83 053 peptides in dormant blastocysts and 101 875 peptides in reactivated blastocysts. Accordingly, a total of 2255 proteins were matched with 1670 proteins in dormant blastocysts and 1978 proteins in reactivated blastocysts (Fig. 1B, Supplemental Table S4). Among these characterized proteins, a total of 277 proteins were detected specifically in dormant blastocysts, whereas 585 proteins were found only in reactivated blastocysts (Fig. 1C, Supplemental Tables S5 and S6).

Considering the protein abundance and reliability of detection in the proteomic profile, approximately 599 differentially expressed proteins were selected for further functional analysis. Among them, 180 proteins were more abundant in dormant blastocysts, whereas the remaining 419 proteins were prominent in reactivated blastocysts (Fig. 1C, Supplemental Table S7). Gene ontology analysis of all detected proteins revealed a similar percentage of identical proteins spanning cellular components and various biological processes between the dormant and reactivated blastocysts (Fig. 1D). However, functional classification analysis of the 599 differentially expressed proteins revealed that 118 proteins were related to mitochondria function, whereas others fell into various other categories such as translation, ribosome, chromatin remodeling, GTPase, regulation of cytoskeleton, endosome transport, and vacuole and lysosome (Fig. 1, E and F, and see Supplemental Table S8 and Supplemental Figs. S1–S6). According to this bioinformatic functional analysis, we next investigated the regulation of various identified basic cellular processes or pathways in dormant versus reactivated blastocysts by means of diverse biological methods.

Increase of Aerobic Glycolysis During Blastocyst Reactivation

Aerobic glycolysis is a process that catalyzes glucose to lactate in the cytoplasm under sufficient oxygen conditions [17]. We found that G6PDX, PKM2, and LDHA, enzymes typical for aerobic glycolysis [18] were significantly upregulated in blastocysts during reactivation, whereas FBP1, an enzyme specific for gluconeogenesis antagonizing glycolysis [19], was downregulated in the reactivated blastocysts (Fig. 2A). The dynamic changes of these genes were further validated by quantitative real-time PCR (Fig. 2B), revealing that these enzymes were upregulated at both the mRNA and protein levels. On the other hand, *Glut1*, a transporter for glucose [20], and *Mct4*, a transporter for lactate [21], exhibited significantly upregulated expression during blastocyst reactivation (Fig. 2C). Immunofluorescence analysis of MCT4 revealed that this protein was substantially elevated in the trophectoderm cells during reactivation (Fig. 2D). Collectively, our results suggested that aerobic glycolytic activities are significantly increased in blastocysts upon reactivation for implantation.

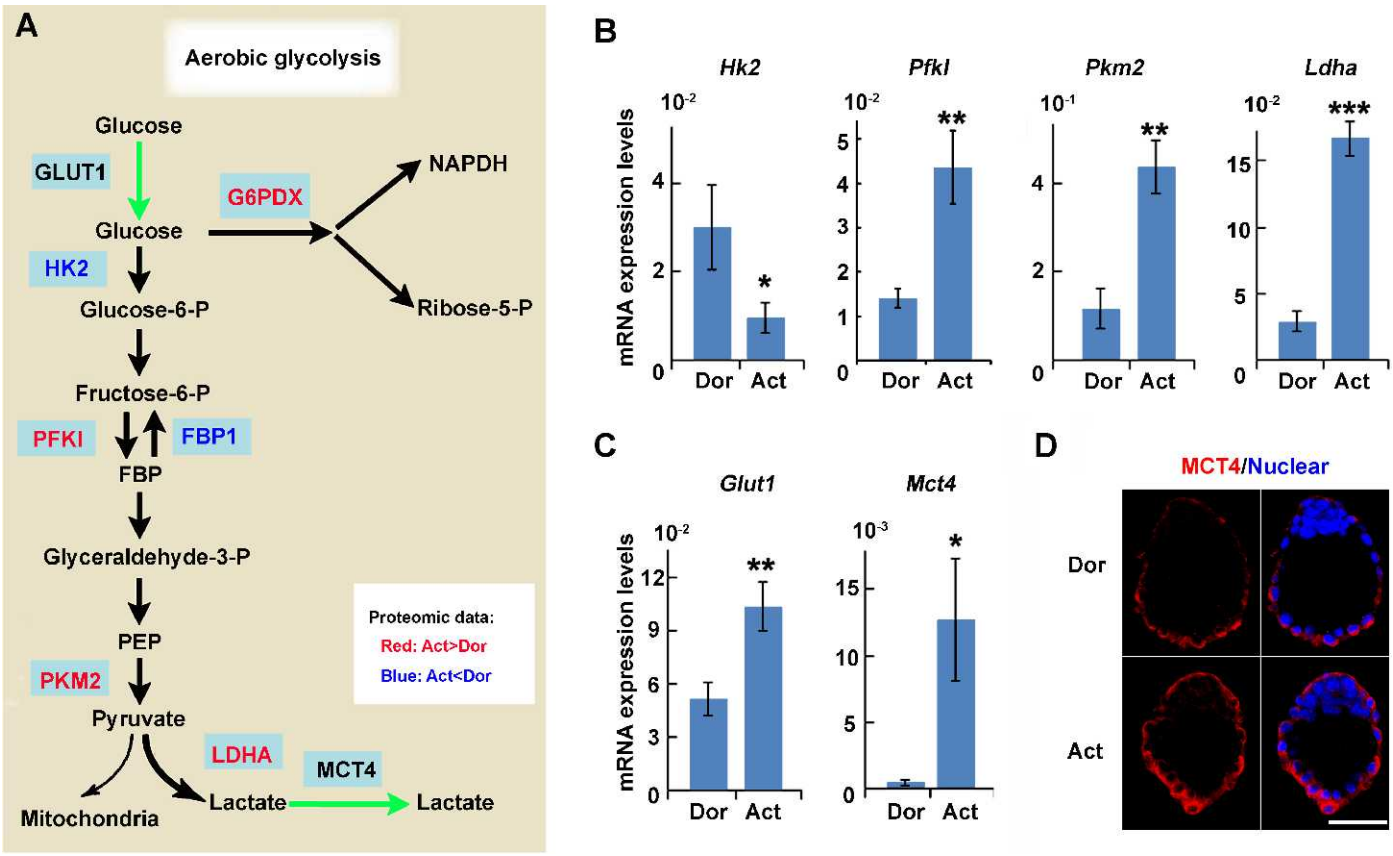

FIG. 2. Regulation of enzymes involved in aerobic glycolysis in blastocysts from dormancy (Dor) to reactivation (Act) is shown. **A**) Key proteins are involved in aerobic glycolysis. Red color shows upregulation of protein levels in reactivated blastocyst, whereas blue shows downregulation. **B**) Detection of gene mRNA expression by quantitative real-time PCR (mean ± SEM). **C**) Detection of *Glut1* and *Mct4* mRNA level was determined by quantitative real-time PCR (mean ± SEM). $*P < 0.05$, $**P < 0.01$, and $***P < 0.001$. **D**) Immunostaining of MCT4 in dormant and reactivated blastocysts shows a global upregulation of this gene in trophectoderm cells. Bar = 50 μm.

Prominent Enhancement of Mitochondrial Function in the Mural Trophectoderm During Blastocyst Reactivation for Implantation

Oxidative phosphorylation coupled with tricarboxylic acid cycle in the mitochondria to produce ATP for most cellular demands. Our proteomic analysis revealed that many enzymes involved in oxidative phosphorylation were differentially expressed in blastocysts undergoing dormancy versus reactivation. For example, whereas COX4I1, COX5A, and COX17 were downregulated, ATP5B, ATP5H, and ATP5L were upregulated in reactivated blastocysts (Fig. 3A), suggesting that ATP production was enhanced in the mitochondria during blastocyst reactivation. Indeed, by measuring the ATP content, we found that ATP production was significantly increased in reactivated blastocysts compared with that in dormant blastocysts (Fig. 3B). This increased ATP production was correlated with a significantly upregulated expression of ATP5B, the catalytic subunit of ATP synthase in the mitochondria [22], with a prominent expression pattern in the mural trophectoderm cells of reactivated blastocysts (Fig. 3, C and D). These results suggested that the mitochondria function for ATP production was mainly increased in mural trophectoderm to support the blastocyst reactivation prior to implantation.

Because the mitochondrial membrane potential ($\Delta\psi_m$) is highly correlated to mitochondria activities [23], we used immunofluorescence monitoring of TMRE, a sensitive indicator for $\Delta\psi_m$ [24]. We found that $\Delta\psi_m$ was present in all trophoblast cells of dormant blastocysts but was dramatically increased in the mural trophectoderm cells of reactivated blastocysts (Fig. 3E), highly consistent with the upregulation of ATP5B expression during blastocyst reactivation. Surprisingly, this increased mitochondrial activity was not caused by altered numbers of mitochondria, as ultrastructural analysis revealed that the total number of mitochondria was statistically comparable in both dormant and reactivated blastocysts (Fig. 3, F and G). Furthermore, we found a significantly decreased number of swollen mitochondria filled with vacuoles in the reactivated blastocysts (Fig. 3, F and H), which would contribute to decreased mitochondria membrane potential because of the opening of the mitochondrial permeability transition pore, as previously reported [25]. Interestingly, the number of swollen mitochondria was also significantly decreased in the inner cell mass during blastocyst reactivation (Fig. 3, F and H), although its physiological relevance needs further investigation. Nonetheless, the results suggested that activation of mitochondria is essential for blastocyst function prior to implantation.

Upregulation of Pentose Phosphate Pathway Coordinates with Purine Nucleotide Biosynthesis in Reactivated Blastocysts

Pentose phosphate pathway directs glucose metabolism to the production of NADPH and ribose for the synthesis of macromolecules and detoxification of reactive oxygen species

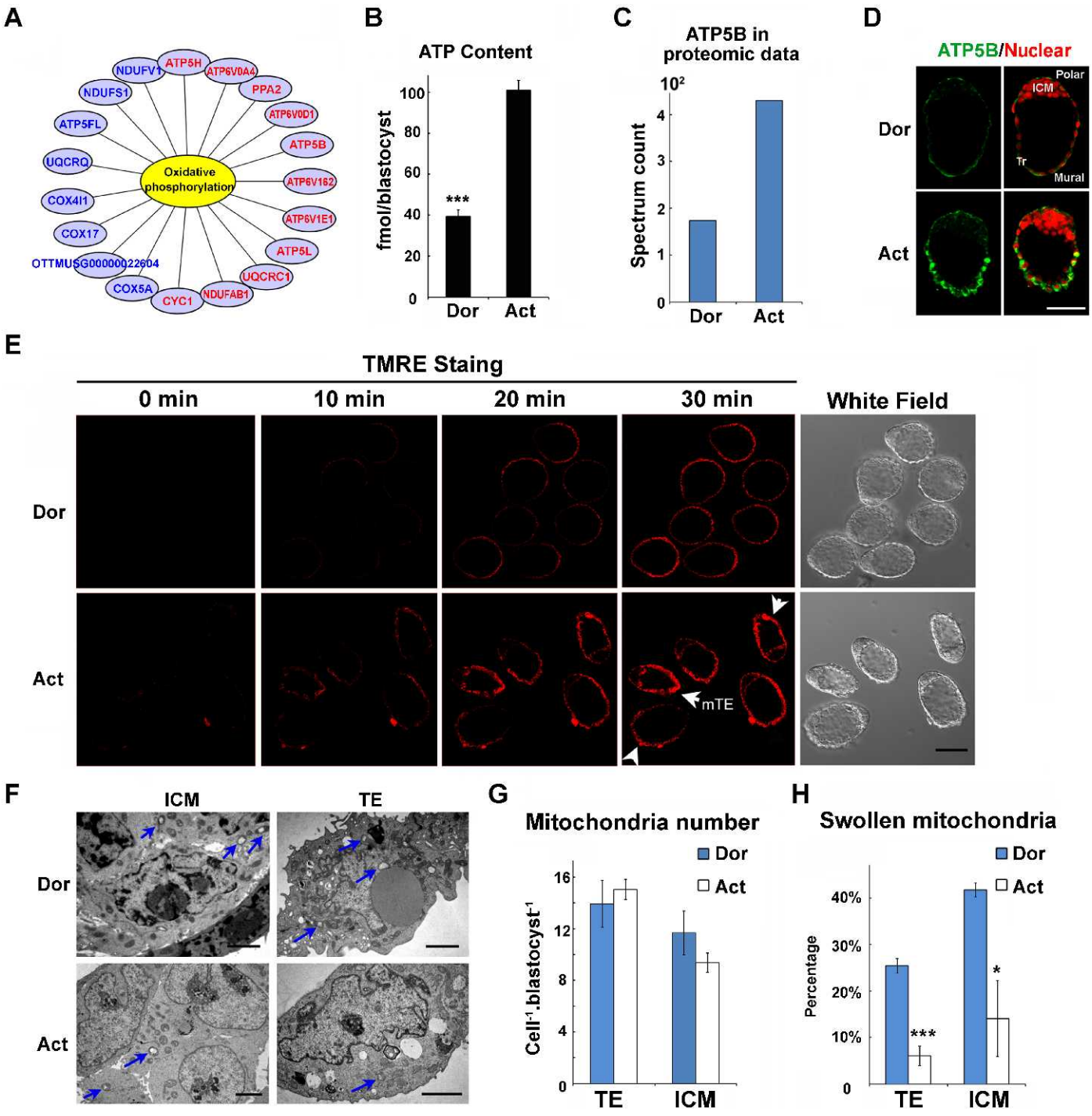

FIG. 3. Mitochondrial function for energy production was significantly enhanced in the mural trophectoderm upon reactivation from dormancy. **A**) Differentially expressed proteins related to oxidative phosphorylation are shown according to their biological process analysis. Red color shows upregulation of protein level in reactivated blastocyst, whereas blue shows downregulation. **B**) ATP content was much higher in reactivated (Act) blastocysts than in dormant (Dor) blastocysts (mean ± SEM). ***$P < 0.001$. **C**) Spectrum counts are shown as protein abundance of ATP5B in proteomic data. **D**) Immunostaining of ATP5B showed significant upregulation of this protein in trophectoderm of reactivated blastocysts. ICM = inner cell mass; TE = trophectoderm. Bar = 50 μm. **E**) Measurement of mitochondria membrane potential is shown by TMRE staining. mTE = mural trophectoderm. Bar = 50 μm. **F**) Mitochondria vacuolization (blue arrow) was frequently observed in dormant blastocysts. Bar = 2 μm. **G**) Average mitochondria numbers were comparable in both dormant and reactivated blastocysts (mean ± SEM). **H**) Quantification of swollen mitochondria is shown in reactivated blastocysts (6.0% in TE and 14.0% in ICM) and dormant blastocysts (25.4% in TE and 41.7% in ICM; mean ± SEM). *$P < 0.05$ and ***$P < 0.001$.

[26]. Glucose-6-phosphate dehydrogenase (G6PDX) is the rate-limiting enzyme of the pentose phosphate pathway [27]. In our study, we found that G6PDX was significantly upregulated in the reactivated blastocysts (Figs. 2A and 4A). In addition to G6PDX, 2 nonreversing enzymes for this process, RPE and TALDO1, also showed significant upregulation. These results suggested an increasing demand for nucleotides and NADPH during blastocyst reactivation. Accompanying activation of the pentose phosphate pathway for ribose-5-P, a major substrate for nucleotide biosynthesis, was the upregulation of a range of

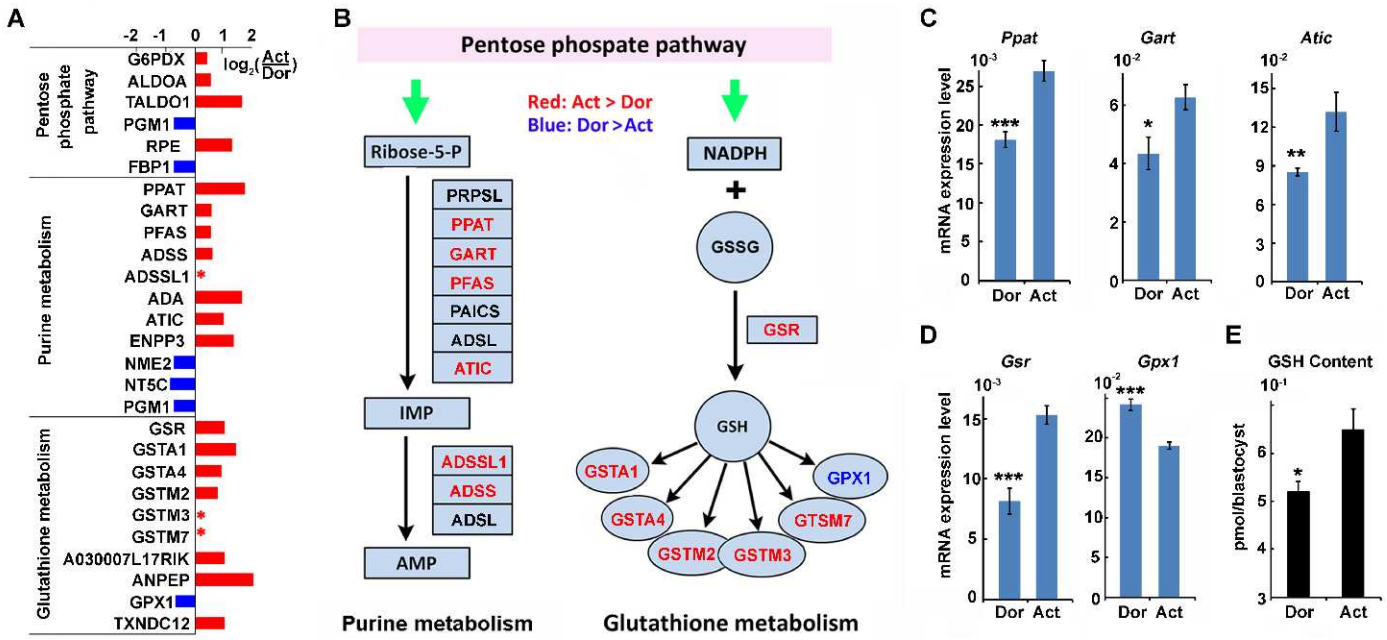

FIG. 4. Upregulation of the pentose phosphate pathway coordinates with increase of purine metabolism and GSH metabolism activities. **A**) Abundance of differentially expressed proteins in pentose phosphate pathway, purine metabolism, and GSH metabolism is shown according to KEGG analysis. *Specific expression in reactivated blastocysts. **B**) Graphs show proteins involved in pentose phosphate pathway, purine metabolism, and GSH metabolism according to KEGG analysis. Red represents upregulated proteins in reactivated blastocyst, whereas blue represents downregulated proteins in reactivated blastocysts. **C**) Detection of mRNA expression of genes involved in purine synthesis is shown (mean ± SEM). **D**) Detection of mRNA expression of genes involved in GSH metabolism is shown (mean ± SEM). **E**) GSH content is shown in dormant (Dor) and reactivated (Act) blastocysts (mean ± SEM). $*P < 0.05$, $**P < 0.01$, and $***P < 0.001$.

enzymes for purine nucleotide biosynthesis, such as PPAT, GART, ATIC, PFAS, ADSS, and ADSSL1 (Fig. 4, A and B). These enzymes also showed upregulated expressions at the transcriptional level by quantitative real-time PCR analysis (Fig. 4C). These observations indicated an increased purine nucleotide biosynthesis during blastocyst reactivation.

Enhanced GSH Metabolism Functions as a Strategy for Cellular Protection During Blastocyst Reactivation

Autophagy has been previously demonstrated to be essential for embryo survival during diapause [28]. However, it remained elusive with respect to the cellular protection machinery during blastocyst reactivation. GSH is the most abundant antioxidant and a major detoxification agent essential for the maintenance of the intracellular redox milieu for the preservation of thiol-disulfide redox states of proteins in living cells [29]. Our proteomic analysis revealed that GSH metabolism was highly activated in the reactivated blastocysts, which may function as a cellular protection strategy during blastocyst reactivation (Fig. 4B). GSR is the key enzyme catalyzing GSSG and NAPDH, a metabolic product of the pentose phosphate pathway, into active GSH [30]. We observed that both mRNA and protein expression of GSR were significantly upregulated in the reactivated blastocysts (Fig. 4, A, B, and D), suggesting an elevation of GSH production during blastocyst reactivation. By measuring the GSH contents in blastocysts, we indeed noted a markedly increased GSH level in reactivated blastocyst compared to dormant blastocysts (Fig. 4E). Accordingly, GSTA1, GSTA4, GSTM2, GSTM3, and GSTM7, key enzymes for GSH to execute its reductive function, were also remarkably upregulated against a robust oxidative stress response during blastocyst reactivation (Fig. 4, A and B). Interestingly, the expression of GSH hydrolytic ectoenzyme ANPEP (also known as aminopeptidase N) [31] was increased in implantation-competent blastocysts (Fig. 4A), highlighting the necessity of GSH homeostasis during blastocyst reactivation for implantation.

Attenuated Leucine Degradation Coordinates with Enhanced Leucine Uptake During Blastocyst Reactivation

It has been reported that the amino acid leucine facilitates trophoblast motility in preimplantation blastocysts [32, 33], ascribing a critical role to leucine during trophoblast differentiation. In the present study, we observed a significantly downregulated expression of IVD, BCKDHB, ABAT, ACAA1A, OXCT1, HADH, and ACADS, key enzymes involved in leucine degradation in reactivated blastocysts (Fig. 5A), suggesting that a high level of leucine is beneficial for blastocyst reactivation in vivo. Downregulation of these genes was also detected at transcriptional levels (Fig. 5B). On the other hand, we noted a remarkably upregulated mRNA expression of *Slc6a14*, a major leucine transporter [32] during blastocyst reactivation (Fig. 5C). Moreover, *Slc6a14* expression was also significantly elevated in Day 5 implanted blastocysts compared to that in Day 4 preimplantation blastocysts (Fig. 5C), indicating an increased leucine uptake during normal blastocyst reactivation. These observations suggested that leucine played an important role during blastocyst reactivation for implantation in vivo: leucine at low levels maintained by active degradation and limited uptake restrains the dormant blastocyst implantation competency, whereas at a higher level, it conduces blastocyst reactivation.

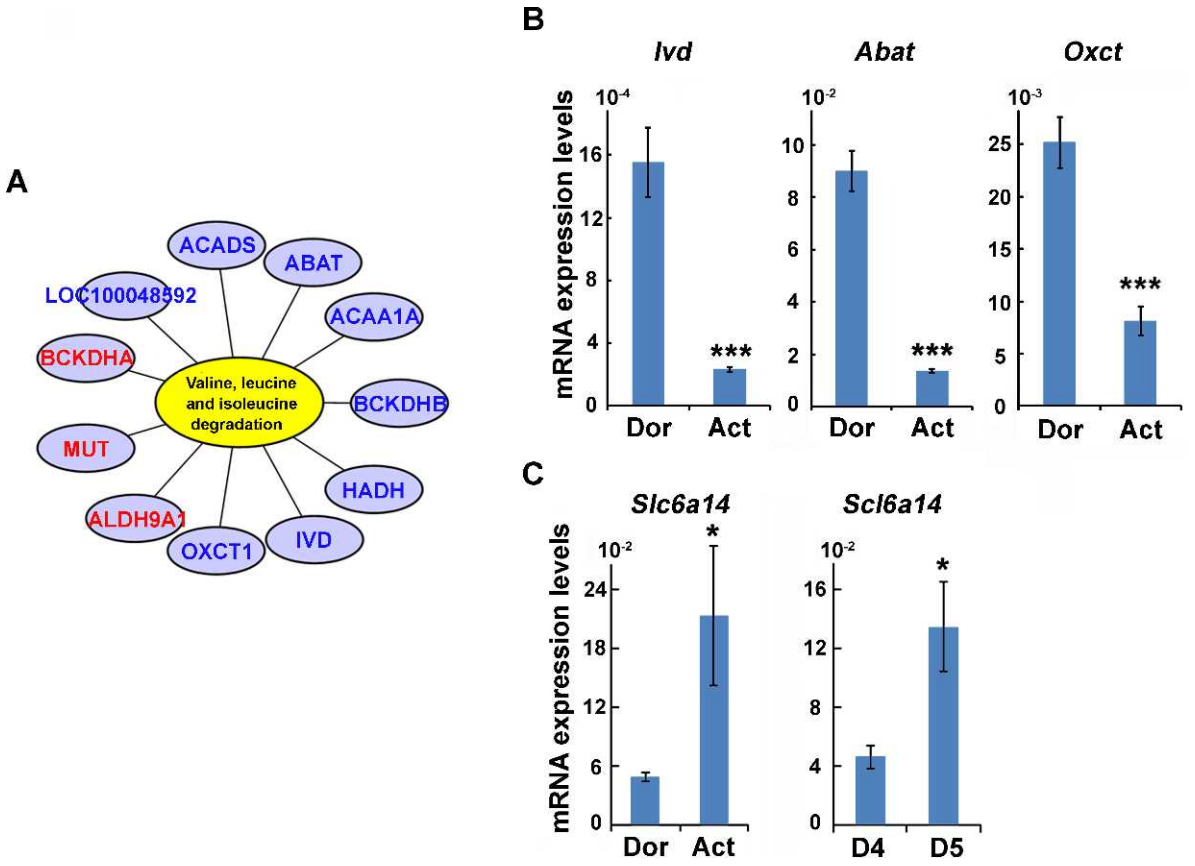

FIG. 5. Regulation of valine, leucine, and isoleucine degradation processes is shown in dormant (Dor) and reactivated (Act) blastocysts. **A**) Proteins differentially expressed in valine, leucine, and isoleucine degradation are shown according to the KEGG pathway analysis. Red color shows upregulation of protein level in reactivated blastocyst, whereas blue shows downregulation. **B**) Detection of mRNA expression of key genes involved in valine, leucine, and isoleucine degradation is shown (mean ± SEM). **C**) Detection of mRNA expression of the leucine transporter *Slc6a14* is shown in reactivated blastocyst versus dormant blastocyst and in E4.5 blastocyst versus E3.5 blastocyst (mean ± SEM). *$P < 0.05$ and *** $P < 0.001$.

Global Nuclear Activity Is Boosted During Blastocyst Reactivation

Previous studies have demonstrated that DNA replication and cell proliferation are restored in blastocysts undergoing reactivation [12, 34, 35], pointing toward a dynamic regulation of nuclear activity during blastocyst reactivation from dormancy. Indeed, our proteomic analysis of dormant versus reactivated blastocysts revealed a wide range of differentially expressed proteins functionally related to chromatin organiza-

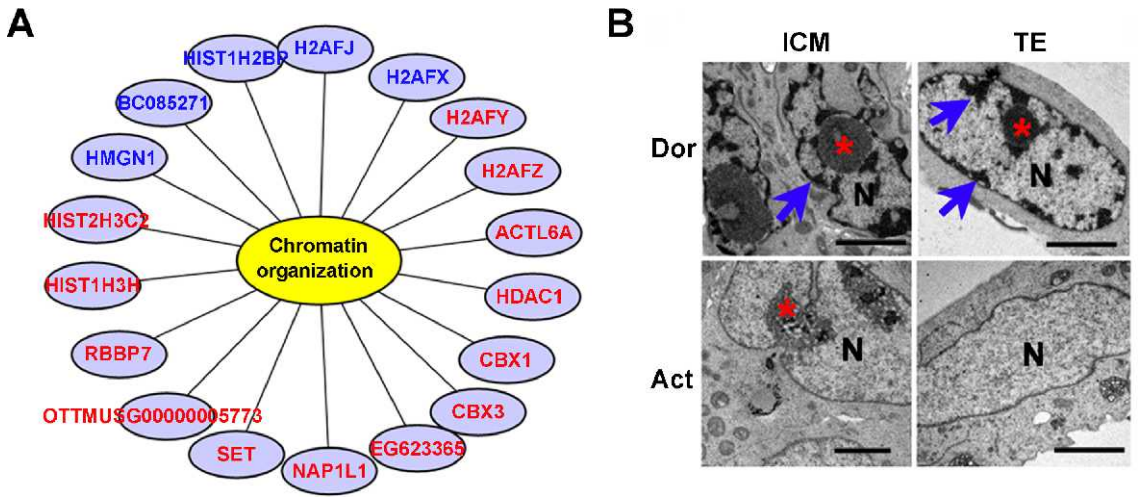

FIG. 6. Regulation of nuclear activities in dormant and reactivated blastocysts is shown. **A**) Proteins differentially expressed in chromatin organization are shown according to functional analysis of their biological processes. Red color shows upregulation of protein level in reactivated blastocyst, whereas blue shows downregulation. **B**) Ultrastructure of nuclei of inner cell mass (ICM) and TE in dormant or activated blastocysts. Dormant blastocyst showed remarkably more heterochromatins (blue arrow) and more condensed nucleoli (red asterisk) in both ICM and TE cells. Bar = 2 μm. N = nucleus.

tion (Fig. 6A). CBX1 and CBX3, also named heterochromatin protein 1 homolog beta and heterochromatin protein 1 gamma, which are critical for chromatin remodeling [36, 37], were found to be differentially regulated (Fig. 6A). H2AFX, the phosphorylation level of which was a typical indicator for the DNA damage-repair activity [38], was found to be increased at the protein level (Fig. 6A), suggesting an increase of DNA replication activity during blastocyst reactivation. Ultrastructural analysis by transmission electronic microscopy further disclosed the differential status of the nucleoli and chromatins in dormant versus reactivated blastocysts (Fig. 6B). The nucleoli, factory for ribosome RNA synthesis, were condensed in dormant blastocysts (Fig. 6B), consistent with the previously reported observation [11]. However, these condensed nucleoli rapidly became loosened 12 h after estrogen injection (Fig. 6B), indicating the restoration of ribosome RNA synthesis for translation activation in reactivated blastocysts. Moreover, the heterochromatin was frequently observed in both the inner cell mass and the trophectoderm cells of dormant blastocysts, whereas the euchromatin was prominent in the reactivated blastocysts (Fig. 6B). Nonetheless, the results collectively pointed toward a remarkable boost of nuclear activity during blastocyst reactivation.

Activation of the Endosome–Lysosome System in the Trophectoderm Is Conducive to Blastocyst Implantation

We identified differential expression of numerous endosome–lysosome-related proteins (Fig. 7A), which are highly associated with cellular endocytosis and phagocytosis activities [39]. For example, we observed that various cathepsins, including CTSB, CTSC, CTSD, and CTSZ, which are localized mainly in endosomes and lysosomes [40], were differentially expressed in the dormant versus the reactivated blastocysts (Fig. 7A). Western blotting of the 2 most highly differentially and abundantly expressed cathepsins, CTSB and CTSD, validated the fact that they were significantly increased in the reactivated blastocysts (Fig. 7B). Using immunofluorescence staining, we further observed that both CTSB and CTSD were upregulated in the trophectoderm, whereas CTSD was selectively expressed in the mural trophectoderm of reactivated blastocysts (Fig. 7C), pointing toward the involvement of cathepsins in trophoblast differentiation during blastocyst reactivation for implantation.

Multivesicular bodies (MVB), which are formed from the late endosomes after fusion with lysosome from endocytosis or phagocytosis [41], notably appeared in the mural trophectoderm of reactivated blastocysts (Fig. 7D). In addition, active phagocytosis of adjacent uterine epithelium cell debris was frequently observed in the mural trophectoderm cells, with a notable amount of MVBs during blastocyst reactivation and attachment (Fig. 7E). These findings suggested that activation of endosome–lysosome system in the mural trophectoderm was highly coordinated with the trophoblast phagocytosis at the maternal-fetal interface during implantation.

DISCUSSION

Embryonic diapause and reactivation is an evolutionary phenomenon ensuring successful pregnancy in nearly 100 species of mammals [4–6]. However, the underlying mechanism governing blastocyst reactivation from diapause remains largely unknown. In the present study, we performed the first integral proteomic analysis of blastocysts to explore the molecular basis that distinguishes blastocyst dormancy from reactivation. Our findings provided herein a global view of the various differentially regulated cellular and molecular processes, including translation processes, aerobic glycolysis, pentose phosphate pathway, purine biosynthesis, GSH metabolism, nuclear activity, cytoskeleton organization, and adhesion molecules in dormant versus reactivated blastocysts. In particular, we revealed timely activation of mitochondria and endosome–lysosome system activities in coordination with the global changes in blastocysts upon reactivation from dormancy, highlighting its physiological significance during blastocyst activation for implantation. Our results furthermore shed light on the underlying machinery distinguishing the blastocyst dormancy and reactivation.

Previous studies have revealed that global energetic activity of dormant blastocysts remained at an extremely low level. This metabolic tranquility of blastocysts rapidly and progressively increases after the reinitiation of implantation mediated by estrogen [42, 43]. Pyruvate uptake increases within 4 h after estrogen-induced reactivation whereas glucose uptake remains basal until 16 h but increases thereafter [44], suggesting that pyruvate may be an important source of energy during the early stage of blastocyst reactivation. In the present study, mitochondria activity was significantly increased particularly in the mural trophectoderm cells, due to changes in mitochondrial morphology but not increase in mitochondria number. This observation was assessable as previous works have shown that mitochondria DNA replication did not occur in oocytes until the blastocyst stage [45, 46], whereas the mitochondrial inner membrane is arranged into transverse cristae in expanded blastocysts with increased oxidative phosphorylation capacity compared to that in earlier stage embryos [47]. We found that swollen mitochondria was significantly decreased in the mural trophectoderm cells, which showed increase of mitochondria membrane potential and ATP5b expression, during blastocyst reactivation. Swollen mitochondria with vacuole reflected the low mitochondria membrane potential due to the opening of the mitochondrial permeability transition pore. It was reported that regulation of mitochondrial permeability transition pore could regulate the intracellular calcium signaling, which would influence preimplantation embryo development and blastocyst adhesion during implantation [48, 49], suggesting that changes in the mitochondrial permeability transition pore are essential for blastocyst reactivation and implantation through regulation of cellular calcium signaling. It has been recently reported that mitochondrion-related transcripts were upregulated during preimplantation embryo development in humans [50]. In fact, mitochondria quality for ATP production has been considered to be a determinant of developmental potential for the oocyte and preimplantation embryos in humans [51].

Nucleotide biosynthesis might be essential for the blastocyst reactivation, as we observed that purine nucleotide synthesis activity was significantly enhanced during blastocyst reactivation. As it has been reported, cell division rate was decelerated within the first 3 days of delayed implantation and with no further significant increase of cell number after Day 7 of delayed implantation [52–54]. Increased DNA synthesis was first noted in the inner cell mass at approximately 6 h after estrogen administration and then in the polar and mural trophoblast cells at approximately 12 to 18 h in vivo [34, 35]. RNA synthesis was persistent during delayed implantation [55], and there was no significant increase of RNA synthesis during the first 24 h of estrogen-induced reactivation [11, 55]. These previously observed results suggested that it might be the DNA synthesis but not the RNA synthesis that urgently demands a large amount of nucleotides during the rapid induction of implantation. Besides, the increase of purine

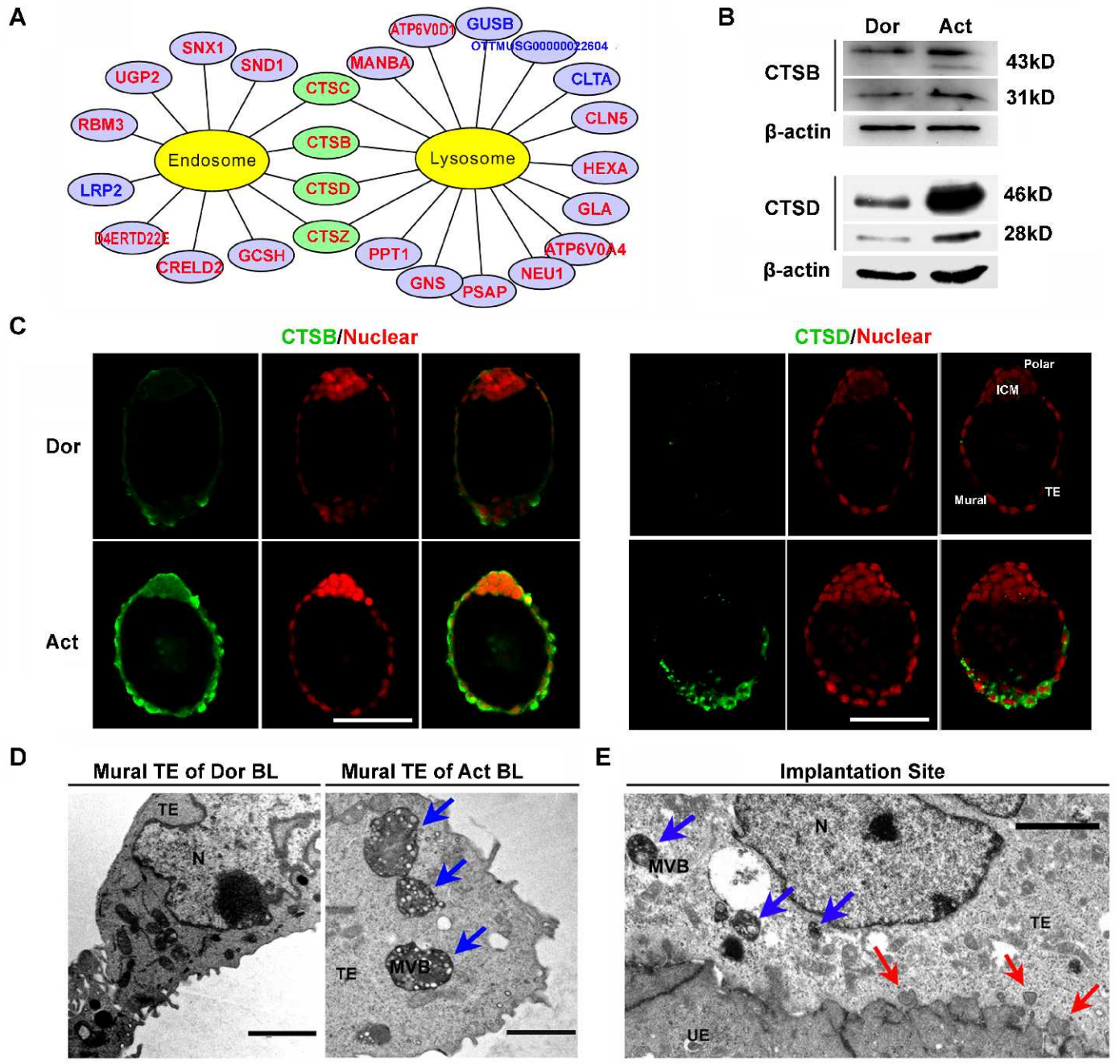

FIG. 7. Timely activation of the endosome–lysosome system in the reactivated blastocyst trophectoderm was coordinated with active phagocytosis at the maternal-fetal interface. **A**) Differentially expressed proteins related to endosome and lysosome from protein profile are shown. Red color shows upregulation of protein level in reactivated blastocyst, whereas blue shows downregulation. **B**) Western blotting of CTSB and CTSD shows a prominent upregulation for both precursors and mature forms in reactivated blastocysts. **C**) Immunostaining of CTSB and CTSD in dormant (Dor) and reactivated (Act) blastocysts is shown. CTSB was globally upregulated in trophectoderm (TE) of reactivated blastocysts; whereas CTSD was specifically upregulated in the mural trophectoderm of reactivated blastocysts. Bar = 50 μm. **D)** Ultrastructure of mural trophoblast cells in dormant and reactivated blastocysts shows a remarkable increase of MVB (blue arrow) in the mural TE of reactivated blastocyst (blue arrow). Bar = 2 μm. N, nucleus. **E**) Ultrastructural analysis is shown of the implantation site in delayed implanting females 12 h after estrogen injection. The adjacent uterine epithelium cells were phagocytosed by mural trophectoderm cells of reactivated blastocyst (red arrow). Bar = 2 μm. N , nucleus; UE, uterine epithelium; blue arrow, MVB.

nucleotide synthesis may also supply cAMP signaling and/or ATP production, as previous work has revealed that activation of cAMP signaling was sufficient for the activation of dormant blastocyst for implantation [56]. However, we failed to detect any enzymes directly involved in pyrimidine metabolism in our proteomic analysis. This unexpected result might be due to the limitation of mass strategy for detection of those enzymes, which belong to macromolecular multifunctional enzymes in the cytoplasm or located on the mitochondrial membrane as previously reported [57–60]. Increase of nuclear activities seemed to be warranted during blastocyst reactivation because previous evidence has shown that global DNA replication was upregulated during the first 24 h of blastocyst reactivation [11, 34, 55]. Surprisingly, the catalog for cell cycles of differentially expressed proteins was not enriched in our proteomic profile.

This was probably due to the limitation of mass strategy for detection of those enzymes which form complexes with DNA.

It has been reported that metabolic activation alone is not sufficient for conferring blastocyst implantation competency [56]. Because blastocyst implantation involves the attachment of the trophectoderm with uterine epithelium and subsequent penetration of trophoblasts through the epithelial layer, one of the central events of blastocyst activation is the trophectoderm differentiation, particularly the achievement of its invasive capacity. Uterine epithelium cells adjacent to the mural trophectoderm die during the penetration of blastocyst from uterine lumen to the stroma [61, 62]. These epithelium cells were probably cleared by the mural trophoblast cells [62–64]. However, it remains unknown what triggered the apoptosis of uterine epithelium cells. In our work, we found that these phagocytic activities of trophoblast cells could be detected as early as 12 h after estrogen-mediated reactivation, when apparent uterine epithelium cell death was rarely detected [61]. It is conceivable that active phagocytosis in mural trophoblast cells would damage the membrane integrity of uterine epithelium cells, therefore facilitating epithelial apoptosis. Besides, it has been shown that cathepsins, such as CTSD, could be secreted as proteases into extracellular matrix for postimplantation trophoblast cell invasion and vascular remodeling [65, 66]. In women, cathepsins were extensively expressed in first trimester placenta, the invasive phase of placentation, indicating the involvement of these proteases in trophoblast invasion [67, 68]. We found that CTSD was significantly increased in mural trophectoderm cells. Thus, cathepsins might also function as secreted proteases during the peri-implantation period for trophoblast invasion.

Nonetheless, in addition to shedding further light on the underlying mechanisms governing blastocyst reactivation from diapause, our findings have high clinical relevance, as activation of mitochondrial function and the endosome–lysosome system are essential for normal preimplantation embryo development and trophoblast invasion during human implantation.

ACKNOWLEDGMENT

We thank Lieqin Liu and Xiaoyan Li for assistance in embryo collection.

REFERENCES

1. Wang H, Dey SK. Roadmap to embryo implantation: clues from mouse models. Nat Rev Genet 2006; 7:185–199.
2. Paria BC, Huet-Hudson YM, Dey SK. Blastocyst's state of activity determines the ''window'' of implantation in the receptive mouse uterus. Proc Natl Acad Sci U S A 1993; 90:10159–10162.
3. Yoshinaga K, Adams CE. Delayed implantation in the spayed, progesterone treated adult mouse. J Reprod Fertil 1966; 12:593–595.
4. Mead RA. Embryonic diapause in vertebrates. J Exp Zool 1993; 266: 629–641.
5. Lopes FL, Desmarais JA, Murphy BD. Embryonic diapause and its regulation. Reproduction 2004; 128:669–678.
6. Renfree MB, Shaw G. Diapause. Annu Rev Physiol 2000; 62:353–375.
7. Murphy BD. Embryonic diapause: advances in understanding the enigma of seasonal delayed implantation. Reprod Domest Anim 2012; 47(suppl 6):S121–S124.
8. Ptak GE, Tacconi E, Czernik M, Toschi P, Modlinski JA, Loi P. Embryonic diapause is conserved across mammals. PLoS One 2012; 7: e33027.
9. Cha J, Sun X, Dey SK. Mechanisms of implantation: strategies for successful pregnancy. Nat Med 2012; 18:1754–1767.
10. Zhang S, Lin H, Kong S, Wang S, Wang H, Armant DR. Physiological and molecular determinants of embryo implantation. Mol Aspects Med 2013; 34:939–980.
11. Van Blerkom J, Chavez DJ, Molecular Bell H. and cellular aspects of facultative delayed implantation in the mouse. Ciba Found Symp 1978; 141–172.
12. Hamatani T, Daikoku T, Wang H, Matsumoto H, Carter MG, Ko MS, Dey SK. Global gene expression analysis identifies molecular pathways distinguishing blastocyst dormancy and activation. Proc Natl Acad Sci U S A 2004; 101:10326–10331.
13. Wang S, Kou Z, Jing Z, Zhang Y, Guo X, Dong M, Wilmut I, Gao S. Proteome of mouse oocytes at different developmental stages. Proc Natl Acad Sci U S A 2010; 107:17639–17644.
14. Wang H, Matsumoto H, Guo Y, Paria BC, Roberts RL, Dey SK. Differential G protein-coupled cannabinoid receptor signaling by anandamide directs blastocyst activation for implantation. Proc Natl Acad Sci U S A 2003; 100:14914–14919.
15. Wang Q, Lu J, Zhang S, Wang S, Wang W, Wang B, Wang F, Chen Q, Duan E, Leitges M, Kispert A, Wang H. Wnt6 is essential for stromal cell proliferation during decidualization in mice. Biol Reprod 2013; 88:5.
16. Lu J, Zhang S, Nakano H, Simmons DG, Wang S, Kong S, Wang Q, Shen L, Tu Z, Wang W, Wang B, Wang H, et al. A positive feedback loop involving Gcm1 and Fzd5 directs chorionic branching morphogenesis in the placenta. PLoS Biol 2013; 11:e1001536.
17. Hsu PP, Sabatini DM. Cancer cell metabolism: Warburg and beyond. Cell 2008; 134:703–707.
18. Bensinger SJ, Christofk HR. New aspects of the Warburg effect in cancer cell biology. Semin Cell Dev Biol 2012; 23:352–361.
19. Zaragoza O, Gancedo JM. Elements from the cAMP signaling pathway are involved in the control of expression of the yeast gluconeogenic gene FBP1. FEBS Lett 2001; 506:262–266.
20. Heilig CW, Concepcion LA, Riser BL, Freytag SO, Zhu M, Cortes P. Overexpression of glucose transporters in rat mesangial cells cultured in a normal glucose milieu mimics the diabetic phenotype. J Clin Invest 1995; 96:1802–1814.
21. Halestrap AP. The SLC16 gene family - structure, role and regulation in health and disease. Mol Aspects Med 2013; 34:337–349.
22. Maguire D, Shah J, McCabe M. Assaying ATP synthase rotor activity. Adv Exp Med Biol 2006; 578:67–72.
23. Yao Z, Gandhi S, Burchell VS, Plun-Favreau H, Wood NW, Abramov AY. Cell metabolism affects selective vulnerability in PINK1-associated Parkinson's disease. J Cell Sci 2011; 124:4194–4202.
24. Collins TJ, Bootman MD. Mitochondria are morphologically heterogeneous within cells. J Exp Biol 2003; 206:1993–2000.
25. Wong PC, Pardo CA, Borchelt DR, Lee MK, Copeland NG, Jenkins NA, Sisodia SS, Cleveland DW, Price DL. An adverse property of a familial ALS-linked SOD1 mutation causes motor neuron disease characterized by vacuolar degeneration of mitochondria. Neuron 1995; 14:1105–1116.
26. Du W, Jiang P, Mancuso A, Stonestrom A, Brewer MD, Minn AJ, Mak TW, Wu M, Yang X. TAp73 enhances the pentose phosphate pathway and supports cell proliferation. Nat Cell Biol 2013; 15:991–1000.
27. Stanton RC. Glucose-6-phosphate dehydrogenase, NADPH, and cell survival. IUBMB Life 2012; 64:362–369.
28. Lee JE, Oh HA, Song H, Jun JH, Roh CR, Xie H, Dey SK, Lim HJ. Autophagy regulates embryonic survival during delayed implantation. Endocrinology 2011; 152:2067–2075.
29. Circu ML, Aw TY. Glutathione and modulation of cell apoptosis. Biochim Biophys Acta 2012; 1823:1767–1777.
30. Choi CH, Kim BJ, Jeong SY, Lee CH, Kim JS, Park SJ, Yim HS, Kang SO. Reduced glutathione levels affect the culmination and cell fate decision in Dictyostelium discoideum. Dev Biol 2006; 295:523–533.
31. Dringen R, Gutterer JM, Gros C, Hirrlinger J. Aminopeptidase N mediates the utilization of the GSH precursor CysGly by cultured neurons. J Neurosci Res 2001; 66:1003–1008.
32. Martin PM, Sutherland AE. Exogenous amino acids regulate trophectoderm differentiation in the mouse blastocyst through an mTOR-dependent pathway. Dev Biol 2001; 240:182–193.
33. Gonzalez IM, Martin PM, Burdsal C, Sloan JL, Mager S, Harris T, Sutherland AE. Leucine and arginine regulate trophoblast motility through mTOR-dependent and independent pathways in the preimplantation mouse embryo. Dev Biol 2012; 361:286–300.
34. Given RL, Weitlauf HM. Resumption of DNA synthesis during activation of delayed implanting mouse blastocysts. J Exp Zool 1981; 218:253–259.
35. Given RL, Weitlauf HM. Resumption of DNA synthesis in delayed implanting mouse blastocysts during activation in vitro. J Exp Zool 1982; 224:111–114.
36. Cheutin T, McNairn AJ, Jenuwein T, Gilbert DM, Singh PB, Misteli T. Maintenance of stable heterochromatin domains by dynamic HP1 binding. Science 2003; 299:721–725.
37. Zeng W, Ball AR, Jr., Yokomori K. HP1: heterochromatin binding proteins working the genome. Epigenetics 2010; 5:287–292.

38. Bonner WM, Redon CE, Dickey JS, Nakamura AJ, Sedelnikova OA, Solier S, Pommier Y. GammaH2AX and cancer. Nat Rev Cancer 2008; 8: 957–967.
39. Itakura E, Kishi-Itakura C, Mizushima N. The hairpin-type tail-anchored SNARE syntaxin 17 targets to autophagosomes for fusion with endosomes/lysosomes. Cell 2012; 151:1256–1269.
40. Haidar B, Kiss RS, Sarov-Blat L, Brunet R, Harder C, McPherson R, Marcel YL. Cathepsin D, a lysosomal protease, regulates ABCA1-mediated lipid efflux. J Biol Chem 2006; 281:39971–39981.
41. Zhang L, Sheng R, Qin Z. The lysosome and neurodegenerative diseases. Acta Biochim Biophys Sin (Shanghai) 2009; 41:437–445.
42. Menke TM, McLaren A. Carbon dioxide production by mouse blastocysts during lactational delay of implantation or after ovariectomy. J Endocrinol 1970; 47:287–294.
43. Nilsson BO, Magnusson C, Widehn S, Hillensjo T. Correlation between blastocyst oxygen consumption and trophoblast cytochrome oxidase reaction at initiation of implantation of delayed mouse blastocysts. J Embryol Exp Morphol 1982; 71:75–82.
44. Spindler RE, Renfree MB, Gardner DK. Carbohydrate uptake by quiescent and reactivated mouse blastocysts. J Exp Zool 1996; 276:132–137.
45. Ebert KM, Liem H, Hecht NB. Mitochondrial DNA in the mouse preimplantation embryo. J Reprod Fertil 1988; 82:145–149.
46. Thundathil J, Filion F, Smith LC. Molecular control of mitochondrial function in preimplantation mouse embryos. Mol Reprod Dev 2005; 71: 405–413.
47. Sathananthan AH, Trounson A. Mitochondrial morphology during preimplantational human embryogenesis. Human Reproduction 2000; 15:148–159.
48. Stachecki JJ, Armant DR. Transient release of calcium from inositol 1,4,5-trisphosphate-specific stores regulates mouse preimplantation development. Development 1996; 122:2485–2496.
49. Rizzuto R, De Stefani D, Raffaello A, Mammucari C. Mitochondria as sensors and regulators of calcium signalling. Nat Rev Mol Cell Biol 2012; 13:566–578.
50. Xue Z, Huang K, Cai C, Cai L, Jiang CY, Feng Y, Liu Z, Zeng Q, Cheng L, Sun YE, Liu JY, Horvath S, et al. Genetic programs in human and mouse early embryos revealed by single-cell RNA sequencing. Nature 2013; 500:593–597.
51. Van Blerkom J. Mitochondrial function in the human oocyte and embryo and their role in developmental competence. Mitochondrion 2011; 11: 797–813.
52. Copp AJ. Effect of implantational delay on cellular proliferation in the mouse blastocyst. J Reprod Fertil 1982; 66:681–685.
53. Paria BC, Das SK, Andrews GK, Dey SK. Expression of the epidermal growth factor receptor gene is regulated in mouse blastocysts during delayed implantation. Proc Natl Acad Sci U S A 1993; 90:55–59.
54. Weitlauf H, Kiessling A, Buschman R. Comparison of DNA polymerase activity and cell division in normal and delayed-implanting mouse embryos. J Exp Zool 1979; 209:467–472.
55. Chavez DJ, Blerkom JV. Persistence of embryonic RNA synthesis during facultative delayed implantation in the mouse. Dev Biol 1979; 70:39–49.
56. Paria BC, Lim H, Wang XN, Liehr J, Das SK, Dey SK. Coordination of differential effects of primary estrogen and catecholestrogen on two distinct targets mediates embryo implantation in the mouse. Endocrinology 1998; 139:5235–5246.
57. Graves LM, Guy HI, Kozlowski P, Huang M, Lazarowski E, Pope RM, Collins MA, Dahlstrand EN, Earp HS, 3rd, Evans DR. Regulation of carbamoyl phosphate synthetase by MAP kinase. Nature 2000; 403: 328–332.
58. Khutornenko AA, Roudko VV, Chernyak BV, Vartapetian AB, Chumakov PM, Evstafieva AG. Pyrimidine biosynthesis links mitochondrial respiration to the p53 pathway. Proc Natl Acad Sci U S A 2010; 107: 12828–12833.
59. Nagaraj N, Wisniewski JR, Geiger T, Cox J, Kircher M, Kelso J, Paabo S, Mann M. Deep proteome and transcriptome mapping of a human cancer cell line. Mol Syst Biol 2011; 7:548.
60. Wisniewski JR, Zougman A, Nagaraj N, Mann M. Universal sample preparation method for proteome analysis. Nat Methods 2009; 6:359–362.
61. El-Shershaby AM, Hinchliffe JR. Epithelial autolysis during implantation of the mouse blastocyst: an ultrastructural study. J Embryol Exp Morphol 1975; 33:1067–1080.
62. Parr EL, Tung HN, Parr MB. Apoptosis as the mode of uterine epithelial cell death during embryo implantation in mice and rats. Biol Reprod 1987; 36:211–225.
63. Welsh AO, Enders AC. Chorioallantoic placenta formation in the rat: I. Luminal epithelial cell death and extracellular matrix modifications in the mesometrial region of implantation chambers. Am J Anat 1991; 192: 215–231.
64. Schlafke S, Welsh AO, Enders AC. Penetration of the basal lamina of the uterine luminal epithelium during implantation in the rat. Anat Rec 1985; 212:47–56.
65. Amarante-Paffaro AM, Hoshida MS, Yokota S, Goncalves CR, Joazeiro PP, Bevilacqua E, Yamada AT. Localization of cathepsins D and B at the maternal-fetal interface and the invasiveness of the trophoblast during the postimplantation period in the mouse. Cells Tissues Organs 2011; 193: 417–425.
66. Screen M, Dean W, Cross JC, Hemberger M. Cathepsin proteases have distinct roles in trophoblast function and vascular remodelling. Development 2008; 135:3311–3320.
67. Divya, Chhikara P, Mahajan VS, Datta Gupta S, Chauhan SS. Differential activity of cathepsin L in human placenta at two different stages of gestation. Placenta 2002; 23:59–64.
68. Hassanein M, Bojja AS, Glazewski L, Lu G, Mason RW. Protein processing by the placental protease, cathepsin P. Mol Hum Reprod 2009; 15:433–442.